JOURNAL OF MATERIALS SCIENCE 14 (1979) 109–124

The structure, modes of deformation and failure, and mechanical properties of diaminodiphenyl sulphone-cured tetraglycidyl 4,4′diaminodiphenyl methane epoxy*

ROGER J. MORGAN†, JAMES E. O'NEAL, DANIEL B. MILLER‡
McDonnell Douglas Research Laboratories, McDonnell Douglas Corporation, St. Louise, Missouri 63166, USA

The tensile mechanical properties of diaminodiphenyl sulphone (DDS) - cured tetraglycidyl 4,4′diaminodiphenyl methane (TGDDM) epoxies [TGDDM-DDS (12 to 35 wt% DDS)] are reported as a function of temperature and strain rate. TGDDM-DDS (20 to 35 wt% DDS) epoxies, which exhibit broad T_gs near 250° C, are not highly cross-linked glasses because diffusional and steric restrictions limit their cross-link density. TGDDM-DDS (10 to 20 wt% DDS) epoxies are more brittle with lower T_gs as a result of lower molecular weights and/or lower cross-link densities. Electron diffraction and X-ray emission spectroscopy studies indicate that TGDDM-DDS (>25 wt% DDS) epoxies contain crystalline regions of unreacted DDS which can be eliminated from these epoxies during cure resulting in microvoids. TGDDM-DDS (12 to 35 wt% DDS) epoxies predominantly deform and fail in tension by crazing, as indicated by fracture topography studies. These glasses also deform by shear banding as indicated by right-angle steps in the fracture topography initiation region and mixed modes of deformation that involve both crazing and shear banding. No evidence was found for heterogeneous cross-link density distributions in TGDDM-DDS (15 to 35 wt% DDS) epoxies on straining films in the electron microscope.

1. Introduction

Epoxies, when utilized as composite matrices and adhesives in aerospace structural components, are often exposed to extreme environments. The durability of epoxies in such environments is difficult to predict without a knowledge of the structure, modes of deformation and failure, and mechanical response relations of these materials and how such relations are modified by fabrication procedures and the service environment. The structure–property relationships of epoxy glasses, however, have received little attention compared with other commonly utilized polymer glasses.

The network structure and microvoid characteristics of epoxies are the primary structural components that control the modes of deformation and failure and mechanical response [1–4].

The network structure of epoxies varies with

*Research sponsored by the Air Force Office of Scientific Research/AFSC, United States Air Force, under Contract No. F44620-76-0075. The United States Government is authorized to reproduce and distribute preprints for governmental purposes notwithstanding any copyright notation hereon.

†Present address: Lawrence Livermore Laboratory, L-338, University of California, P.O. Box 808, Livermore, Ca 94550, USA.

‡National Science Foundation Faculty Research Participant: NSF Grant No. SER 76-04721. Present address: Physical Science Division, Forest Park Community College, St. Louis, Missouri, USA.

© *1979 Chapman and Hall Ltd. Printed in Great Britain.*

chemical composition and cure conditions. Generally, the cure reactions and final network structure of epoxies have been estimated from (a) the chemistry of the system, if the cure reactions were known and assumed to go to completion, and (b) experimental techniques such as infra-red spectroscopy, swelling, dynamic mechanical, thermal conductivity, differential scanning calorimetry, viscosity, and dielectrometry measurements [5–22]. However, in certain epoxy systems, the chemical reactions may be diffusion-controlled and never go to completion, and a heterogeneous distribution in the cross-link density may also occur. For certain cure conditions, high cross-link density regions from 6 to 10^4 nm in diameter have been observed in cross-linked resins [1–4, 7, 23–44]. The conditions for formation of a heterogeneous rather than a homogeneous system depend on polymerization conditions (i.e., temperature, solvent and/or chemical composition). The ordered regions have been described as agglomerates of colloidal particles [28, 29] or floccules [31] in a lower molecular weight interstitial fluid. Solomon *et al.* [30] suggested that a two-phase system is produced by microgelation prior to the formation of a macrogel. These microgel regions may originate in the initial stages of polymerization from the formation of micro-regions of aggregates of primary polymer chains [40, 45]. Kenyon and Nielsen [7] suggested that the highly cross-linked microgel regions are loosely connected during the latter stages of the cure process. Heterogeneities also can result from either configurational restrictions leading to excessive intramolecular cross-linking [46] or from the chemical composition of the epoxy network formed at a given time being different from that of the chemical composition of the monomer mixture [47]. The high cross-link density regions have been reported to be only weakly attached to the surrounding matrix [28, 29, 31], and their size varies with cure conditions [28], proximity of surfaces [31, 41], and the presence of solvents [7, 30].

Recently, we have studied the network structure of diethylene triamine (DETA)-cured bisphenol-A-diglycidyl ether (DGEBA) epoxies by straining films directly in the electron microscope [3]. These epoxies were found to consist of 6 to 9 nm diameter particles which remain intact when flow occurs. We suggest that these particles are intramolecularly cross-linked, molecular domains. The 6 to 9 nm diameter particles interconnect to form larger 20 to 35 nm diameter aggregates which are observed in patches on surfaces and in thin films of DGEBA–DETA epoxies. Two types of network structures were observed in these studies: (a) regions of high cross-link density embedded in a low- or non-cross-linked matrix and (b) low- or non-cross-linked density regions embedded in a high cross-link density matrix.

Microvoids in epoxies act as stress concentrators and sinks for sorbed moisture and will, therefore, deteriorate the mechanical response. These microvoids can be formed during cure as a result of evolution of trapped, low molecular weight material. The low molecular weight material may be air, moisture, or clusters of unreacted epoxy constituents. The latter may result from inhomogeneous mixing and/or microscopic phase separation of the constituents prior to or during cure. For example, the ability of DGEBA epoxide monomer to crystallize as a separate phase in polyamide-cured DGEBA epoxies has been shown to subsequently cause microvoids in these epoxies for certain cure conditions [1, 2, 4].

The relation between the network structure, microvoid characteristics and failure processes of epoxies has received little attention. Localized plastic flow has been reported to occur during the deformation and failure of epoxies [1–4, 34, 36, 48–54], and in a number of cases, the fracture energies have been reported to be a factor of two to three times greater than the expected theoretical estimate for purely brittle fracture [36, 48, 49, 53–64].

Recent studies revealed that the mode of deformation and failure in DGEBA–DETA epoxy films either strained directly in the electron microscope or strained on a metal substrate is a crazing process [3]. The fracture topographies of bulk DGEBA–DETA epoxy glasses fractured as a function of temperature and strain rate were also interpreted in terms of a crazing process. The flow processes that occurred within craze fibrils during deformation of DGEBA–DETA epoxy films strained in the electron microscope depended on the network structure. Deformation of the network consisting of high cross-link density particles embedded in a deformable, low cross-link density matrix occurred by preferential deformation of the low cross-link density regions without causing cleavage of the high cross-link density regions. However, deformation of the network consisting of low cross-link density regions embedded in a

high cross-link density matrix involved network cleavage and flow in the high cross-link density regions simultaneously as flow with little network cleavage occurred in the neighbouring low cross-link density regions.

In this study, our objective was to characterize further the structure/deformation/mechanical property relations of epoxies. The amine-cured tetrafunctional epoxide studied was tetraglycidyl 4,4′diaminodiphenyl methane epoxide (TGDDM) cured with diaminodiphenyl sulphone (DDS). This epoxy system is currently one of the most commonly utilized in the aerospace industry. A series of epoxies was cured from different TGDDM–DDS compositions, and the tensile mechanical properties were monitored as a function of test temperature and strain rate. The structure and microvoid characteristics were monitored by (a) X-ray emission spectroscopy measurements, (b) electron diffraction measurements, and (c) weight-loss/moisture-sorption studies as a function of anneal temperature. Fracture topography studies were utilized to monitor the modes of deformation and failure of these glasses. In addition, epoxy films were strained directly in the electron microscope to further elucidate the structure of these epoxies.

2. Experimental

2.1. Materials and sample preparation

The epoxy system studied was a diaminodiphenyl sulphone (Ciba Geigy, Eporal)-cured tetraglycidyl 4,4′diaminodiphenyl methane (Ciba Geigy, MY720) epoxy (TGDDM–DDS). The structure of the unreacted TGDDM epoxide and DDS monomers are illustrated in Fig. 1. The TGDDM epoxide monomer is a liquid at room temperature, whereas

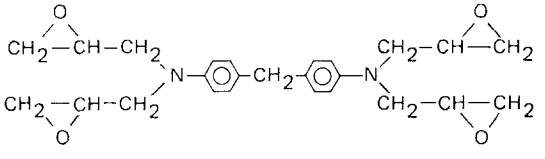

tetraglycidyl 4, 4′ diaminodiphenyl methane epoxy
TGDDM

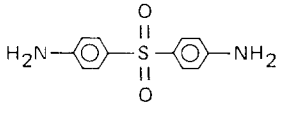

4, 4′ diaminodiphenyl sulfone
DDS

Figure 1 The TGDDM–DDS epoxy system.

the DDS is a crystalline powder with a melting point of 162° C.

For sample preparation, the fabrication techniques developed by Fanter [65] were utilized. A master batch of TGDDM was heated to 75° C, and the DDS was added slowly while the mixture was stirred. This mixture was then held at 75° C for 3 h, periodically stirred, and poured into vials and stored at −20° C. TGDDM-DDS mixtures were prepared in the 10 to 35 wt% DDS range. (For TGDDM–DDS mixtures containing $\gtrsim$30 wt% DDS, the solid DDS did not all dissolve using this procedure; it did dissolve at the higher temperatures utilized during cure.)

Table I illustrates the percentage by weight of DDS required for (1) all primary and secondary amines in the DDS to react and (2) only primary amines in the DDS to react with 50 or 100% of the epoxide groups in the tetrafunctional TGDDM molecules.

In order to prepare dumb-bell-shaped specimens suitable for tensile mechanical property studies, the TGDDM–DDS mixture was heated to 165° C. After 20 min at 165° C, the mixture was degassed in a vacuum chamber, reheated to 165° C, and then poured into dumb-bell-shaped silicone rubber moulds. The specimens were cured at 150° C for 1 h, followed by 5 h at 177° C, cooled to room temperature, and removed from the moulds. The specimens had a gauge length of 3.0 cm, a width of 0.4 cm within the gauge length, and a thickness of 0.6 mm.

Epoxy films, ~ 1 μm thick, suitable for straining directly in the electron microscope, were prepared between salt crystals. The cure conditions were similar to those utilized in preparing the dumb-bell-shaped specimens. After cure, the crystals were dissolved in water, and the film was washed with distilled water. Specimens, 2 mm square, were cut from the epoxy film. Thinner, 100 nm thick films were prepared by a similar procedure for electron diffraction and bright-field transmission studies.

Dumb-bell-shaped specimens were also used for weight loss/moisture sorption studies.

2.2. Experimental procedure

A table model tensile tester (Instron TM-S-1130) was used to determine the tensile mechanical properties of the TGDDM–DDS epoxies in the 10^{-2} to 10^{1} min^{-1} strain rate region from 23 to 265° C.

A scanning reflection electron microscope (JEOL model JEM-100B) and optical microscope (Zeiss Ultraphot II) were used for fracture topo-

TABLE I Theoretical reaction mixtures for TGDDM–DDS epoxy system

	100% TGDDM epoxide groups react	50% TGDDM epoxide groups react
100% DDS primary and secondary amines react	37 wt % DDS	23 wt % DDS
100% DDS primary amines react	54 wt % DDS	37 wt % DDS

graphy studies, For the electron microscope studies, the fracture surfaces were coated with gold while the sample was rotated in vacuum.

For the X-ray emission spectroscopy (XES) studies, uncoated fracture surfaces were exposed to the electron beam, and the surface was scanned for X-rays characteristic of sulphur. The sulphur distribution (as indicated by the relative concentration of white dots) is superimposed on a secondary electron micrograph of the fractured surface. A lithium-drifted silicon X-ray detector (Kevex) was utilized in conjunction with a data analysis system (Tracor Northern).

Bright-field transmission electron microscopy (TEM) was used to monitor the morphology of $\sim 1\,\mu$m thick films that were strained directly in the electron microscope. The 2 mm square, epoxy specimens were fastened to standard cartridge specimen holders with cement (Duco, E. I. DuPont). The specimen holder was attached to an EM-SEH specimen elongation holder which was introduced into the microscope via the side-entry goniometer. The specimens were deformed in the microscope at a strain rate of $\sim 10^{-2}$ min^{-1}. Selected area electron diffraction studies were also performed on thinner, ~ 100 nm thick films using the microscope in the electron diffraction mode.

Weight loss/moisture sorption measurements were performed by annealing specimens in a tube furnace in a He atmosphere for 24 h. The specimens were weighed before and after annealing and again after a 3 h exposure to steam in a 120° C autoclave.

3. Results and discussion

3.1. Mechanical properties

The tensile mechanical properties of the TGDDM–DDS epoxies were determined as a function of composition (12 to 35 wt % DDS) and temperature (23 to 265° C) at a strain rate of $\sim 10^{-2}$ min^{-1}. In Figs. 2, 3, and 4 the tensile strengths, ultimate elongations, and Young's moduli are plotted as a function of temperature for TGDDM–DDS (12 to 35 wt % DDS) epoxies. The decreases in tensile strengths and moduli and increase in ultimate elongations with increasing temperature from 200 to 250° C for TGDDM–DDS (23 to 35 wt % DDS) epoxies indicate that these glasses exhibit broad glass transitions near 250° C. The 10 to 17% ultimate elongations exhibited by the TGDDM–DDS (23 to 35 wt % DDS) epoxies from 200 to 250° C suggests that these glasses are not highly cross-linked despite the tetrafunctionality of the TGDDM epoxide. TGDDM–DDS (10 to 20 wt % DDS) epoxies exhibit lower T_gs and corresponding softer mechanical properties at lower temperatures than those epoxies prepared from higher DDS concentrations. The TGDDM–DDS (12 wt % DDS) epoxy exhibits $<10\%$ ultimate elongation near its T_g, thus indicating that a more brittle, lower molecular weight epoxy is formed with ~ 10 wt % DDS than is formed at higher DDS concentrations.

A plot of T_g as a function of initial DDS concentration, shown in Fig. 5, confirms that TGDDM–DDS epoxies are not highly cross-linked. [The temperatures representative of the broad T_gs were taken as those temperatures at which the room temperature modulus (E_{RT}) decreased by half (i.e., $E_{RT}/2$).] From 10 to 25 wt % DDS, the

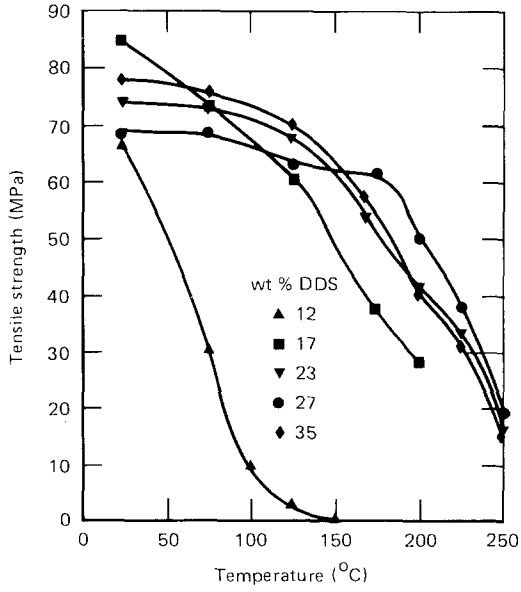

Figure 2 Tensile strength (± 2 MPa) (strain rate $\sim 10^{-2}$ min^{-1}) versus temperature for TGDDM–DDS (12 to 35 wt % DDS) epoxies.

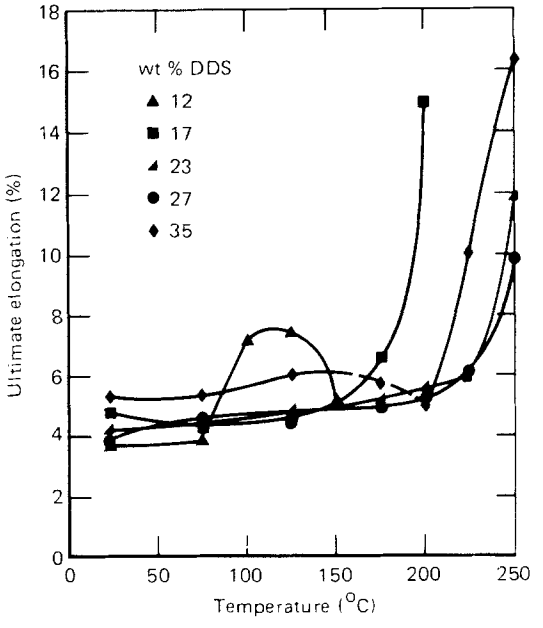

Figure 3 Ultimate elongation (±0.2%)(strain rate $\sim 10^{-2}$ min^{-1}) versus temperature for TGDDM–DDS (12 to 35 wt% DDS) epoxies.

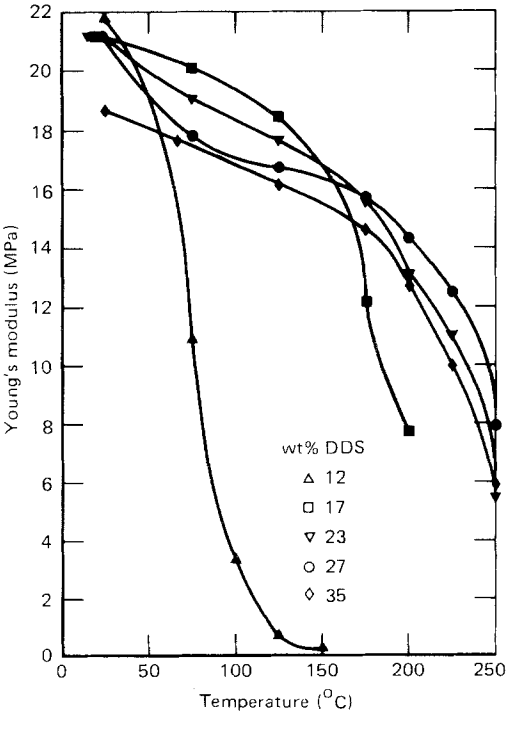

Figure 4 Young's modulus (±1 MPa)(strain rate $\sim 10^{-2}$ min^{-1}) versus temperature for TGDDM–DDS (12 to 35 wt% DDS) epoxies.

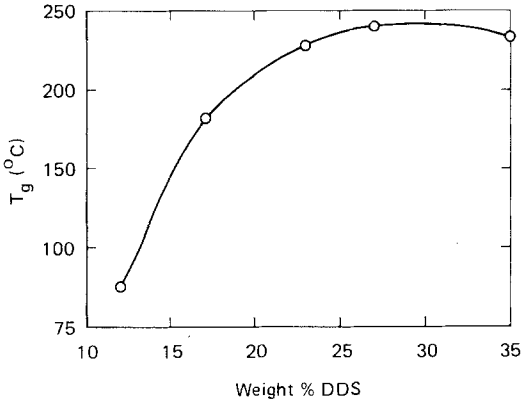

Figure 5 T_g versus initial wt% of DDS in TGDDM–DDS epoxies.

T_g rises with increasing DDS concentration because of corresponding increases in molecular weight and/or cross-link density. The T_g exhibits a maximum of $\sim 250°$ C at ~ 30 wt% DDS and subsequently decreases for higher DDS concentrations. For epoxies prepared from $\gtrsim 25$ wt% DDS, steric and diffusional restrictions evidently inhibit additional epoxy–amine reactions. Examinations of molecular models of the tetrafunctional TGDDM molecule indicate that the epoxide groups are sterically restricted which inhibits their ability to react with the primary amine hydrogens of the DDS. In addition, after gelation at the cure temperature, unreacted groups have difficulty approaching one another spatially because of mobility restrictions produced by the glassy state and the network cross-links. Above ~ 30 wt% DDS concentrations, unreacted DDS molecules plasticize the epoxy system and decrease the T_g (evidence for the presence of unreacted DDS molecules in these epoxies is presented in Sections 3.2 and 3.3). However, 37 wt% DDS is required to consume half the TGDDM epoxide groups when only epoxide–primary amine reactions occur (Table I). Hence, the maximum in T_g at ~ 30 wt% DDS suggests that less than half the TGDDM epoxide groups have reacted when only epoxide–primary amine reactions occur and steric and diffusional restrictions inhibit further reactions. It seems doubtful that networks in which only half of the epoxide groups have reacted would exhibit the respectable mechanical properties shown by the TGDDM–DDS (20 to 35 wt% DDS) epoxies. Evidently, other cure reactions, in addition to the epoxide–primary amine reactions, are occurring and possibly involve (1) epoxide homopolymerization, (2) epoxide–

secondary amine reactions and (3) internal cyclization within the TGDDM epoxide as a result of hydoxyl and/or secondary amines reacting with adjacent unreacted epoxides.

In the $(T_g - 50)$ to T_g temperature range, TGDDM–DDS (17 to 35 wt% DDS) expoxies exhibit definite yield stresses where the stress remains constant with increasing strain. The strain rate dependence of the yield stress in this temperature range was investigated for TGDDM–DDS (27 wt% DDS) epoxy to determine if the data for this cross-linked glass fit Eyring's theory of stress-activated viscous flow for polymers [66]. This theory predicts [67] that the yield stress (σ_y) is a linear function of the logarithm of the strain rate ($\dot{\epsilon}$) at constant temperature T, i.e.,

$$\frac{d\sigma_y}{d \ln \dot{\epsilon}} = \frac{2kT}{v}, \quad (1)$$

where k is Boltzmann's constant and v is the activation volume which is associated with that volume displaced when a chain segment jumps when acted upon by an applied stress. The data for TGDDM–DDS (27 wt% DDS) epoxy fit the Eyring model as illustrated by the linear plots of σ_y versus log $\dot{\epsilon}$ at 225, 250 and 265° C in Fig. 6. The values of the activation volume at each temperature are shown in Table II and are within the range of values (i.e., $v = 3$ to 15 nm^3) reported for non-cross-linked polymers [68–74] and one cross-linked epoxy resin system [75]. These observations suggest that either regions of low cross-link density control the flow processes of this epoxy near T_g and/or the rupturing of cross-links does not significantly affect the activation volume in this temperature range.

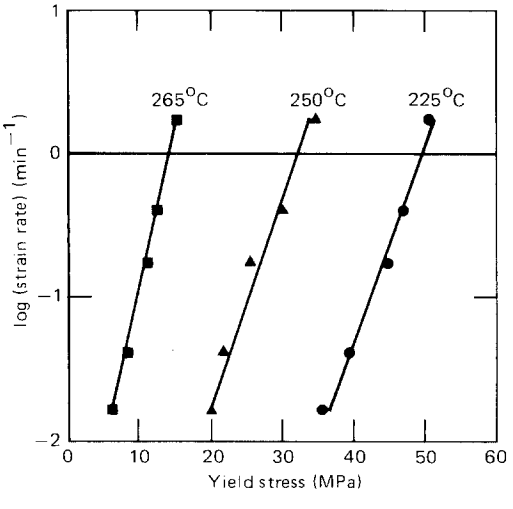

Figure 6 Log (strain rate) versus yield stress for TGDDM–DDS (27 wt% DDS) epoxy as a function of temperature.

TABLE II

Temperature (° C)	Activation volume, v (nm)^3
225	8.0
250	7.9
265	11.7

The larger value of the activation volume at 265° C compared with values at the lower temperatures may be a result of additional cross-links which form during testing. At 265° C, the epoxy rapidly discolours because of the formation of free radicals [4] associated with complex oxidative cross-linking reactions. (The enhanced mobility of the epoxy at 265° C allows such reactions to occur rapidly.) Hence, this larger value of the activation volume suggests that an increase in cross-link density will significantly increase the activation volume. However, such an interpretation must be treated with caution because the physical meaning of v on a molecular level is still unclear [67].

3.2. Electron diffraction

The data presented in Section 3.1 suggest that unreacted DDS molecules may be present in TGDDM–DDS ($\lesssim$ 25 wt% DDS) epoxies. Previous studies on polyamide-cured bisphenol-A-diglycidyl ether epoxies have shown that unreacted epoxide monomer can recrystallize in the partially cured resin [4]. Hence, electron diffraction studies were performed on TGDDM–DDS ($\lesssim$25 wt% DDS) epoxy films to determine if any liquid clusters of unreacted DDS molecules recrystallized within these glasses.

Several electron diffraction patterns of DDS powder on a carbon film were produced. A typical selected area diffraction (SAD) pattern illustrating a polycrystalline pattern of DDS is shown in Fig. 7a. For a hexagonal form, the unit cell dimensions of DDS were determined to be $a = 0.526$ nm and $c = 1.236$ nm. From these unit cell dimensions, a complete list of interplanar spacings was calculated to obtain a standard pattern for DDS.

TGDDM–DDS ($\lesssim$25 wt% DDS) epoxy films exhibited electron diffraction patterns from isolated regions. Such regions, which were $\lesssim 1\ \mu$m in size, appeared as dark but indistinct regions in bright field transmission electron micrographs. The SAD pattern originating from such a region is illustrated in Fig. 7b. The interplanar spacing determined from this pattern agreed with those of the calculated standard DDS pattern, indicating that

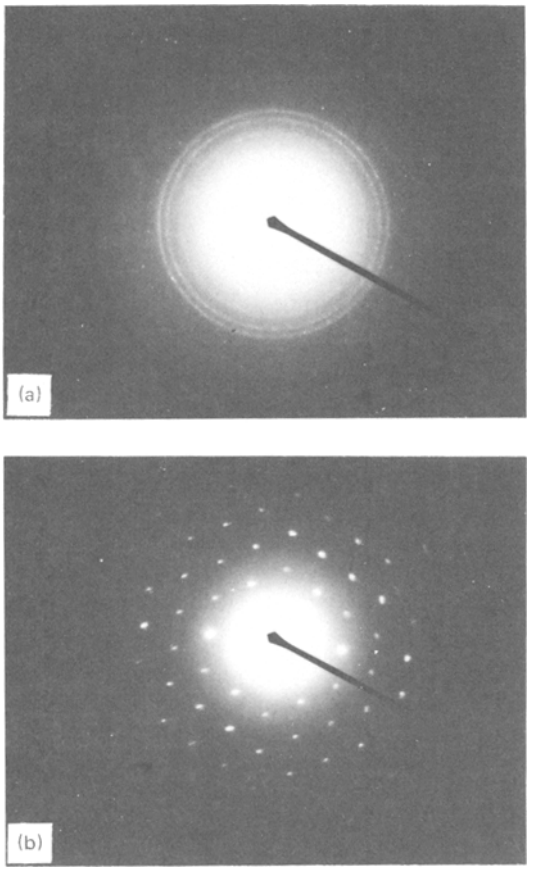

Figure 7 Selected area electron diffraction pattern of (a) DDS powder (polycrystalline) and (b) unreacted DDS crystalline region in TGDDM–DDS (35 wt % DDS) epoxy.

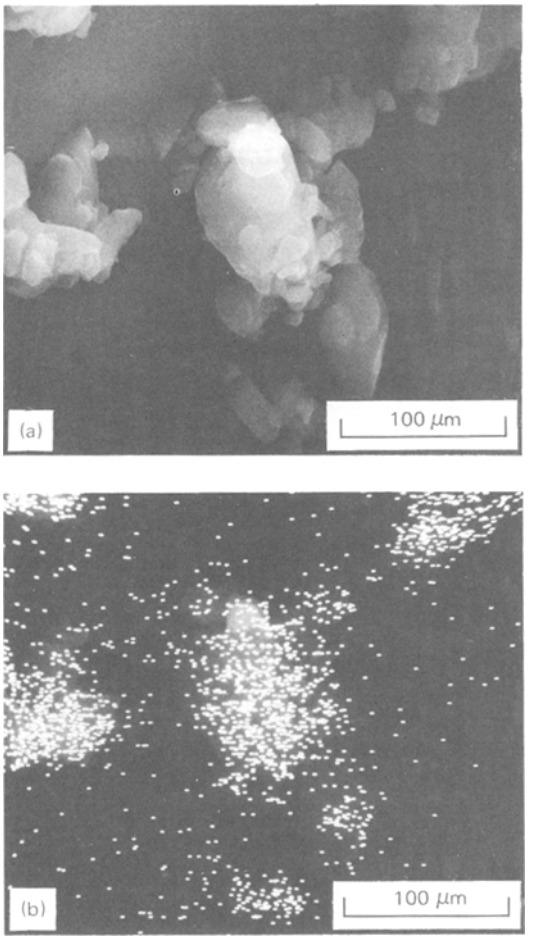

Figure 8 (a) Scanning electron micrograph of DDS crystalline powder and (b) X-ray emission scanning spectroscopy map of sulphur distribution in the same micrograph.

DDS crystalline regions are present in the TGDDM–DDS ($\lesssim$ 25 wt % DDS) epoxy films.

3.3. X-ray emission spectroscopy

X-ray emission spectroscopy (XES) studies were conducted on TGDDM–DDS ($\lesssim$ 25 wt % DDS) epoxies to detect regions of high sulphur content. The detection of such regions would imply the presence of unreacted DDS clusters because sulphur atoms are present only in the DDS molecule (see Fig. 1).

In this technique a fracture surface is bombarded with an electron beam, and the surface is scanned for X-rays characteristic of sulphur. The validity of XES to detect concentrations of DDS was established by monitoring DDS crystalline powder which was sprinkled onto a carbon background. A scanning electron micrograph of such DDS particles is shown in Fig. 8a. The sulphur distribution (as indicated by the relative concentration of white dots) is superimposed on this micrograph in Fig. 8b, thus illustrating that particles of DDS $\gtrsim 10\,\mu$m in size can be detected by this technique. Similar regions were observed in isolated areas of the fracture surfaces of TGDDM–DDS ($\lesssim$ 25 wt % DDS) epoxies. In Fig. 9 an XES map of the sulphur distribution in the fracture surface of TGDDM–DDS (27 wt % DDS) epoxy is illustrated. The large concentration of sulphur in the fracture-initiation region probably results from a cluster of unreacted DDS molecules which acted as a site for craze/crack initiation. Regions $\lesssim 10\,\mu$m in size were not detected by this technique.

XES was also evaluated as a technique to monitor chemically different regions of polymers, such as cross-link density distribution, in the 10 nm size range. From extensive studies on TGDDM–DDS epoxies and polycarbonate–siloxane block copolymers, we have concluded that this technique

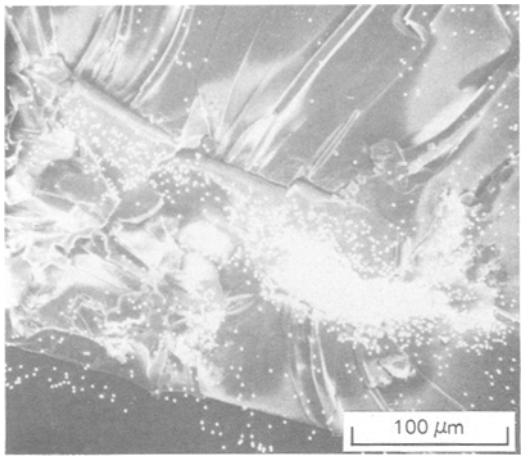

Figure 9 X-ray emission scanning spectroscopy map of sulphur distribution in the fracture surface of TGDDM–DDS (27 wt% DDS) epoxy.

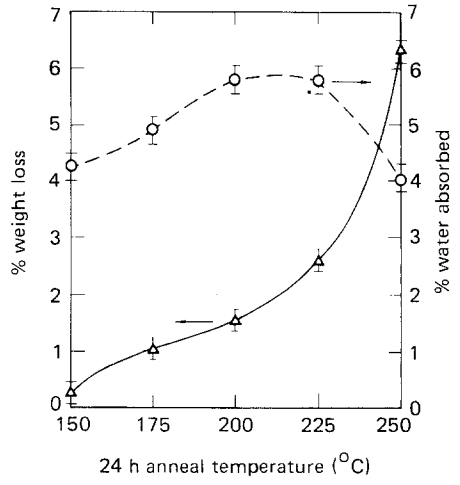

Figure 10 Plots of weight loss and subsequent moisture sorption versus anneal temperature for TGDDM–DDS (27 wt% DDS) epoxy.

is sensitive only to distinct, $\gtrsim 10\,\mu m$ sized, chemically different regions in polymers.

3.4. Weight loss/moisture sorption measurements

We have shown by optical microscopy that unreacted islands of epoxide monomer present in amide-cured bisphenol-A-diglycidyl ether epoxies can produce microvoids by diffusing out of these epoxies when they are annealed below T_g [4]. Microvoids are undesirable in epoxies because they act as stress concentrators, and also serve as a sink for sorbed moisture which deteriorates the mechanical integrity [76]. The weight lost and the subsequent moisture sorbed by TGDDM–DDS (27 wt% DDS) epoxy, as a function of a 24 h anneal from 150 to 250° C, were measured to determine if any clusters of unreacted DDS were eliminated from this epoxy, thus producing microvoids. The production of microvoids is expected to cause an increase in the amount of moisture sorbed by the epoxy. (Optical microscopy was not used in these studies because the size of the DDS clusters was generally $< 1\,\mu m$ and, hence, any microvoids formed from such clusters would be too small to be detected by this technique.)

Fig. 10 shows the progressive weight loss with increasing anneal temperatures from 150 to 250° C for the TGDDM–DDS (27 wt% DDS) epoxy which was originally cured at 177° C for 5 h. The amount of moisture subsequently sorbed by the epoxy at 120° C in an autoclave for 3 h after annealing at 150 to 250° C is plotted versus anneal temperature. The increase in sorbed moisture with increasing anneal temperature from 150 to 200° C is associated with microvoids produced by the elimination of unreacted DDS clusters. The sorbed moisture exhibits a maximum at 200 to 225° C and decreases as the anneal temperature approaches T_g at ~245° C. We associate this maximum and the subsequent decrease in moisture sorption with the enhanced mobility of the epoxy at these higher temperatures, causing a partial collapsing of the microvoids and a possible increase in the crosslink density. Both of these phenomena will decrease the moisture sorption capabilities of the epoxy.

Hence, it is possible that once TGDDM–DDS ($\gtrsim$25 wt% DDS) epoxies form glasses at their cure temperatures, subsequent curing can cause elimination of unreacted clusters of DDS resulting in microvoids.

3.5. Fracture topography studies

The fracture topographies of TGDDM–DDS (12 to 35 wt% DDS) epoxies were studied by optical and scanning electron microscopy as a function of temperature and strain rate. Three characteristic topographic regions were observed in these epoxies: (1) a coarse initiation cavity, (2) a slow crack growth, smooth, mirror-like region, and (3) a fast crack growth, rough region. The fracture topography features were generally similar to those observed in our studies of amine- and amide-cured disphenol-A-diglycidyl ether epoxies [3, 4] and can be interpreted in terms of a crazing deformation and failure process. However, the TGDDM–DDS

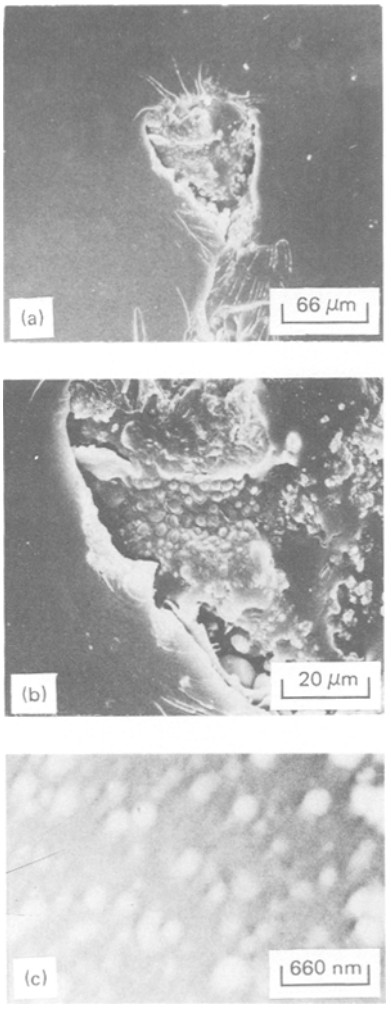

Figure 11 Scanning electron micrographs of (a) overall fracture topography initiation cavity, (b) coarse fractured fibrils and (c) fine fractured fibrils in TGDDM–DDS (27 wt% DDS) epoxy, fractured at room temperature at a strain rate of 10^{-2} min^{-1}.

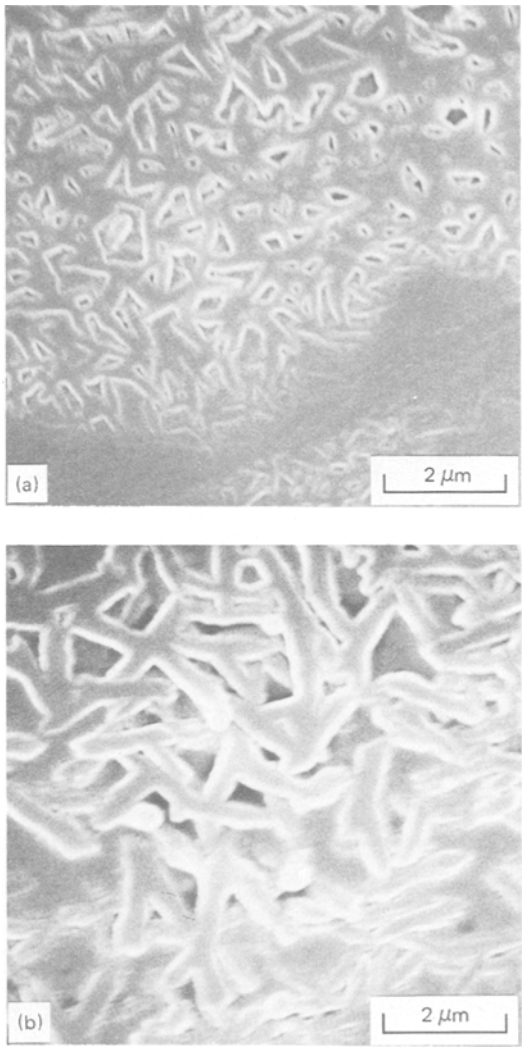

Figure 12 Scanning electron micrographs of fibrils swept onto the fracture surface in TGDDM–DDS (23 wt% DDS) epoxy, fractured at 200° C at a strain rate of 10^{-2} min^{-1}.

fracture topography initiation regions also exhibit unique features as a result of shear-band deformation which occurs in ~ 20% of room temperature fractured specimens. These unique topographical features will be considered later in this section.

A typical fracture topography initiation region characteristic of a TGDDM–DDS epoxy that deformed and failed by a crazing process is illustrated in Fig. 11. The overall fracture topography initiation cavity is illustrated in Fig. 11a; 1 to 5 μm diameter, poorly developed, fractured fibrils are shown in Fig. 11b, and well-developed, 100 to 200 nm diameter, finer fractured fibrils are illustrated in Fig. 11c. This coarse initiation region results from void growth and coalescence through the centre of a simultaneously growing, poorly developed craze, which generally consists of coarse fibrils [3, 4, 77–81]. The diameters of the fractured fibrils depend on the relative rates of craze and void growth. These relative rates vary for different stages of craze–crack growth and depend on complex local stress fields which change from specimen to specimen because of different flaw characteristics. Above 100° C, the fracture topography initiation regions are smoother than at lower temperatures because the enhanced mobility of the glass allows relaxation of the topographical features. Elongated fibrils that have been swept

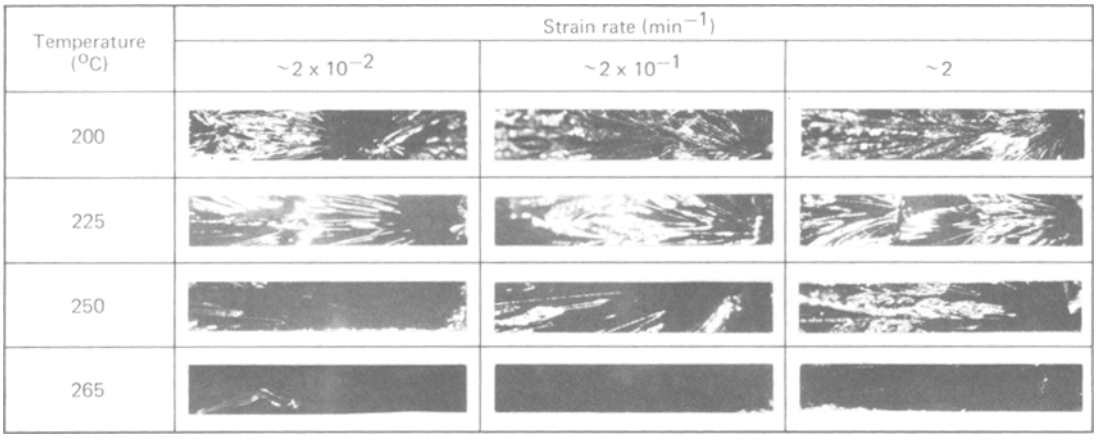

Figure 13 Optical micrographs of overall fracture topographies of TGDDM–DDS (27 wt % DDS) epoxies as a function of temperature and strain rate.

onto the fracture surface as the crack passes through the craze were also observed in the fracture topography initiation region and immediate surroundings for specimens fractured at $\gtrsim 100^\circ$ C, as illustrated in Fig. 12. Similar topographies of fractured fibrils that lie parallel to the surface have been reported by Doyle [82, 83] and Hoare and Hull [84] for polystyrene and by the authors for DGEBA–DETA epoxies [3].

The smooth mirror-like region of the fracture topography of TGDDM–DDS epoxies whose area increases with increasing temperature and decreasing strain rate (Fig. 13) can be attributed to a crazing process. Similar observations have been reported for DGEBA–DETA epoxies [3]. For other polymers, this region has been associated with slow crack growth, and its size varies with temperature, molecular weight and strain rate [85–89]. For polyester resins, Owen and Rose [90] report that the mirror-like area increases with resin flexibility. This smooth topography is associated with slow crack propagation through the median or along the craze–matrix boundary interface of a thick, well-developed craze consisting of fine fibrils [77, 78, 83, 84, 91–95]. Furthermore the increased mobility of the glass near T_g enhances relaxation of the topographical features, thus also favouring a smooth surface.

Interference colours, often observed in the mirror-like region of non-cross-linked polymer glasses [96], were not evident in the fracture topography of TGDDM–DDS epoxies. The absence of such colours in other cross-linked polymers [3, 4, 48] suggests that the thickness of the craze or craze remnants in the mirror-like regions of these cross-linked glasses was not large enough to cause interference with visible light.

The TGDDM–DDS epoxies also deform to a limited extent by shear banding. Regular, right-angle steps were observed in the fracture topography initiation region, all illustrated in Fig. 14. The topography of the right-angle steps exhibits a finer structure at higher magnifications as shown in Fig. 15 where both faces of a right-angle step and their line of intersection are illustrated. Attached to each face is a thin, deformed layer (~ 100 nm thick) of material that consists of rectangular or square-shaped voids and protrusions with dimensions of 100 to 500 nm. These structures are aligned parallel to the line at which the larger perpendicular planes intersect. This topography suggests that the larger shear bands consist of packets of micro-shear bands whose thickness of ~ 100 nm is that of the larger bands. Wu and Li [97] have characterized two shear band deformation processes in polystyrene; one appears as fine shear bands and the other as diffuse shear zones. Also, for shear bands that propagate in epoxies under compression, Bowden and Jukes [98] report that the matrix material outside the bands does not undergo any permanent plastic deformation. Certainly, a sharp boundary between the deformed material in a shear band and the undeformed immediate surroundings is consistent with the thin layer of deformed material observed in the shear planes in Fig. 15.

The percentage of all fractures in which regular right-angle steps were prevalent in the initiation region is plotted as a function of test temperature in Fig. 16. At and above 250° C ($T_g \simeq 250^\circ$ C), none

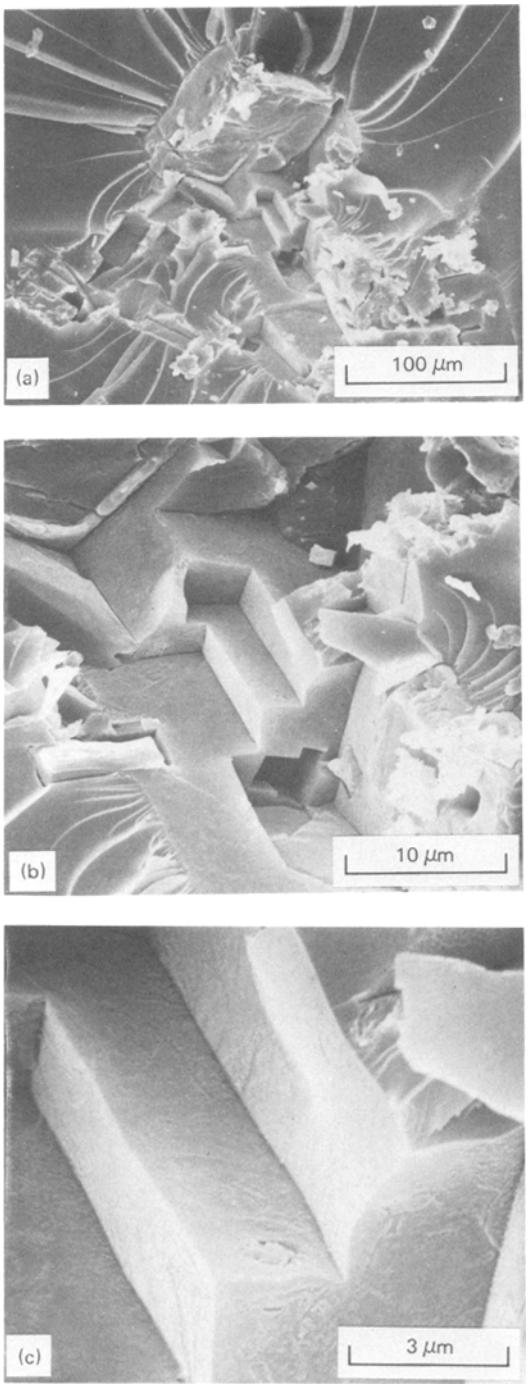

Figure 14 Scanning electron micrographs of right-angle steps in the fracture topography initiation region of TGDDM–DDS (35 wt% DDS) epoxy fractured at 225° C at a strain rate of 10^{-2} min^{-1}.

of the fracture surfaces exhibited the right-angle steps because viscous flow and relaxation processes during and after crack propagation cause a smooth fracture surface and mask the fracture topography

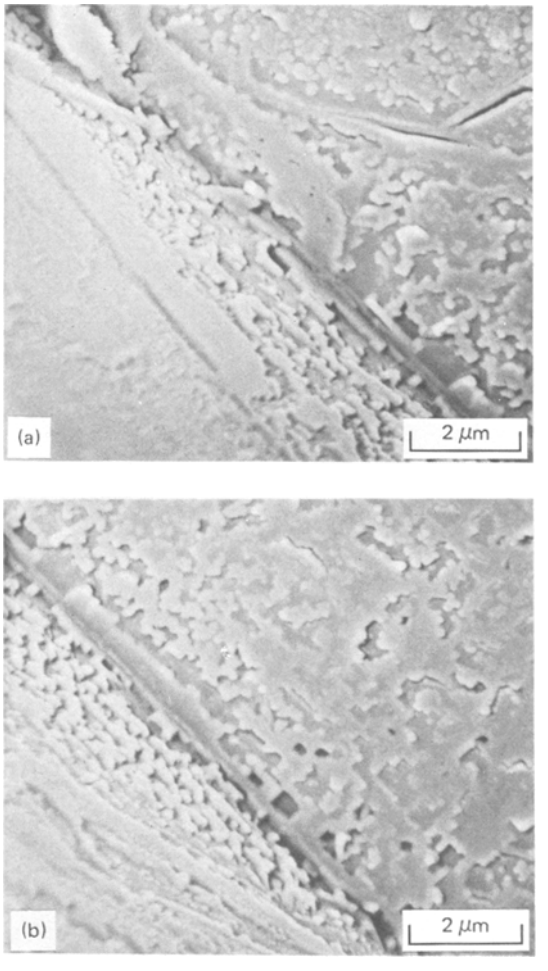

Figure 15 Scanning electron micrographs of the fine structure exhibited at the intersection of both faces of a right-angle step in the fracture topography intiation region of TGDDM–DDS (27 wt% DDS) epoxy fractured at 225° C at a strain rate of $1\ min^{-1}$.

microfeatures. The increase in the percentage of fracture topographies exhibiting right-angle steps with temperature is consistent with the shear band mode of deformation becoming more favoured relative to the crazing mode with increasing temperature [99–101]. Also, Bowden [67] has noted that the rate at which shear bands develop is controlled by the rate of strain softening and the strain rate sensitivity of the flow stress. The relatively low magnitudes of $d\sigma_y/d\ln\dot{\epsilon}$ of 2.5 to 3.5 $MN\,m^{-2}$ for TGDDM–DDS epoxies above 200° C (ascertained from Fig. 6) compared with values quoted for poly(methyl methacrylate) of 5 to 9 $MN\,m^{-2}$ [67] suggest that shear band deformation is favourable for TGDDM–DDS epoxies above 200° C.

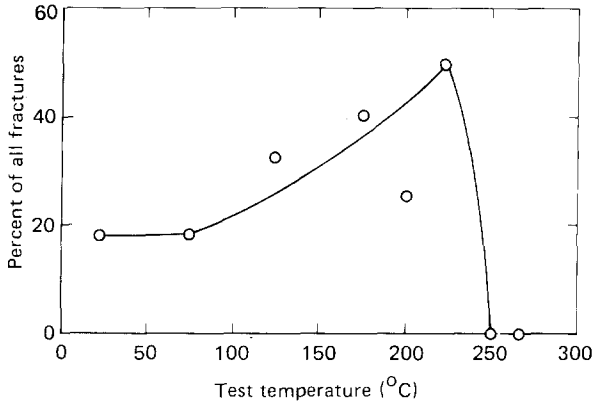

Figure 16 Percentage of fracture topography initiation regions that exhibit right-angle steps versus temperature in TGDDM–DDS (15 to 35 wt% DDS) epoxies.

Shear bands, which propagate at 45° to the applied tensile load direction and therefore intersect at right-angles, produce structurally weak planes in cross-linked glasses because of bond cleavage that is caused during molecular flow. Hull [102] and Mills [103] have both noted that the intersection of shear bands causes a stress concentration that is sufficient to cause a crack to propagate through the thin, structurally weak planes caused by shear band propagation. These phenomena produce the unique right-angle steps in the fracture topography of TGDDM–DDS epoxies that have not yet been observed in any other polymeric materials. Generally, the planes of the shear bands were ~45° to the applied tensile load direction. However, in some cases, significant deviations from the 45° angle were observed because of complex, local stress fields in the fracture initiation region.

The fracture topography initiation regions that exhibited right-angle steps were surrounded by a smooth, mirror-like topography region. At lower temperatures this region is associated with craze propagation [77, 78, 83, 84, 91–95]. Hence, at faster crack velocities, the initial mode of deformation that was predominantly a shear band mode changes to a crazing mode.

The ability of TGDDM–DDS epoxies to deform by shear banding, particularly near T_g, allows these glasses to exhibit the high-temperature ultimate elongations illustrated in Fig. 3. In comparison, for certain polyimides that deform only by crazing [104], the ultimate elongation decreases with increasing temperature because the softening of the craze fibrils limits their load-bearing capability, enhances crack propagation, and thus limits the ultimate elongation. The shear-band deformation in TGDDM–DDS epoxies, however, enhances the

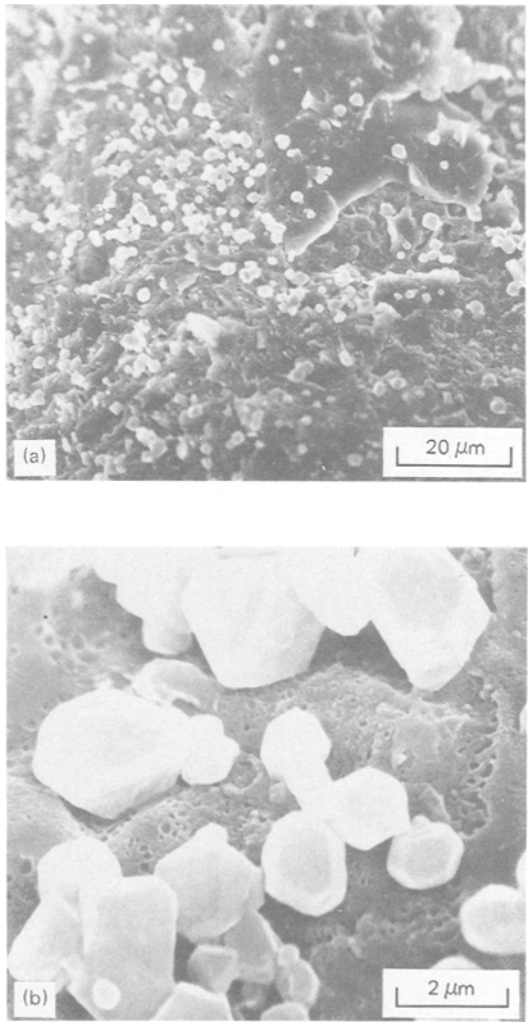

Figure 17 Scanning electron micrographs of regularly-shaped structures embedded in the porous craze fracture topography initiation region of a TGDDM–DDS (23 wt% DDS) epoxy, which was fractured at room temperature at a strain rate of ~ 10^{-2} min^{-1}.

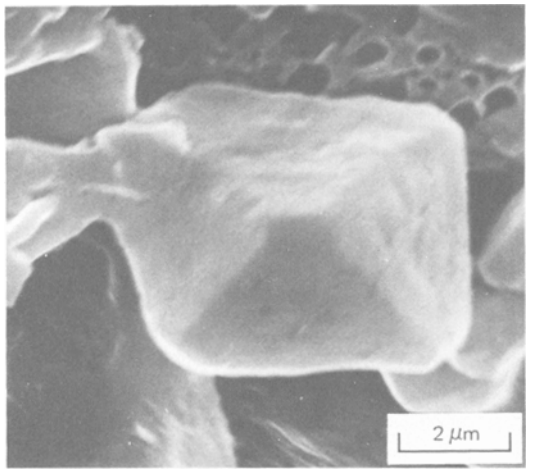

Figure 18 Scanning electron micrograph of regularly shaped structure embedded in the porous craze fracture topography initiation region of a TGDDM–DDS (12 wt% DDS) epoxy, which was fractured at 75° C at a strain rate of $\sim 10^{-2}$ min^{-1}.

high-temperature ductility without leading to premature failure.

In the fracture topography initiation region, regularly-shaped structures occasionally were found embedded in the porous craze structure as illustrated in Figs. 17 and 18. Such structures are not crystallites of unreacted DDS, for the following reasons: (1) such regular shapes were not observed in the micrographs of unreacted DDS powder (Fig. 8a); (2) clusters of these structures $\lesssim 10\,\mu$m in size did not exhibit higher sulphur contents than their surroundings as determined by XES; and (3) these regular structures were observed in TGDDM–DDS (12 wt% DDS) epoxies, whereas regions of unreacted DDS were found only in TGDDM–DDS ($\lesssim 25$ wt% DDS) epoxies (Sections 3.2 and 3.3). In addition, it is difficult to envisage such regularly-shaped regions of high cross-link density, which would be less susceptible to deformation than their surroundings, being present in these TGDDM–DDS epoxies. The most plausible explanation of these regularly-shaped structures is a result of a mixed mode of deformation in which numerous shear bands develop in a region where craze growth also occurs. Perpendicular cracks develop where shear bands intersect at right-angles, and these cracks interconnect with neighbouring perpendicular cracks to produce the assortment of regular structures illustrated in Figs. 17 and 18. The variety of regular structures, most of which contain some perpendicular planes, results from the numerous three-dimensional positions that perpendicular shear bands can have relative to neighbouring shear bands which also meet at right-angles. The complex nature of the local stress fields in this mixed deformation mode could further complicate the situation by producing local deviations of the shear band planes from the $\sim 45°$ angle to the applied tensile load direction.

3.6. Films strained directly in the electron microscope

Significant information on the failure processes and structure of DGEBA–DETA epoxies was found from bright-field transmission electron micrographs of $\sim 1\,\mu$m thick epoxy films strained directly in the microscope [4]. Similar studies were conducted on TGDDM–DDS (10 to 35 wt% DDS) epoxies. On straining TGDDM–DDS epoxies in the electron microscope, cracks propagated rapidly without detection of crazing or shear band modes of deformation. However, prior to crack propagation, microscopic heterogeneities were observed in the more brittle epoxies prepared from 10 to 15 wt% DDS which possess poorer network structures than epoxies prepared from higher DDS concentrations. In Fig. 19a, a strained TGDDM–DDS (10 wt% DDS) epoxy is shown to break into 2.5 to 13 nm diameter particles. At higher deformation, the network breaks into ~ 2.5 nm dia-

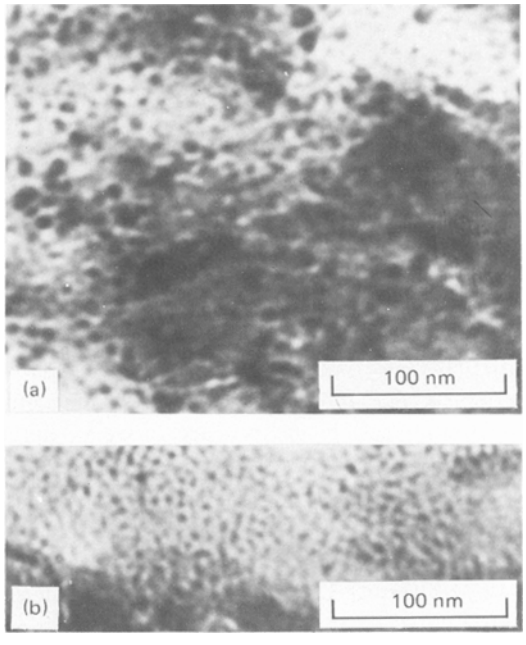

Figure 19 Bright-field transmission electron micrographs of structure in deformed TGDDM–DDS (10 wt% DDS) epoxy.

meter particles, as shown in Fig. 19b. These basic 2.5 nm diameter particles are of a similar size as the TGDDM epoxide molecule. The lack of any heterogenieties in the TGDDS–DDS (15 to 35 wt% DDS) epoxies suggests that these epoxies possess a uniform cross-link density distribution. The symmetry of the tetrafunctional TGDDM epoxide molecule would favour such a uniform distribution for a network formed as a result of primary amine/epoxide reactions.

4. Conclusions

(1) TGDDM–DDS (20 to 35 wt% DDS) epoxies, which exhibit broad T_gs near 250° C, are not highly cross-linked glasses as indicated by (a) their glassy state, high-temperature ductility and (b) the values of their activation volumes associated with the flow processes which are similar to non-cross-linked polymer glasses. Diffusional and steric restrictions inhibit the formation of high cross-link density TGDDM–DDS epoxies despite the tetrafunctionality of the TGDDM epoxide. TGDDM–DDS (10 to 20 wt% DDS) epoxies exhibit progressively lower T_gs and more brittle mechanical responses with decreasing DDS concentrations as a result of low molecular weight and/or low cross-link densities.

(2) Electron diffraction and X-ray emission spectroscopy studies indicate that TGDDM–DDS ($\lesssim$ 25 wt% DDS) epoxies contain crystalline regions of unreacted DDS as a result of steric and diffusional restrictions limiting the cure reactions. Such DDS clusters can be eliminated from these epoxies during the cure process resulting in microvoids in the glasses.

(3) TGDDM–DDS (12 to 35 wt% DDS) epoxies predominantly deform and fail in tension by a crazing process as indicated by fracture topography studies. These glasses also deform to a limited extent by shear banding as indicated by unique, regular right-angle steps in the fracture topography initiation region. The shear band mode of deformation becomes more predominant with increasing temperature and is the primary mode of deformation during the initial stages of fracture just below T_g. Fracture topographical features also indicate that mixed modes of deformation that involve both shear banding and crazing can occur in these epoxies. The shear-band mode of deformation enhances the high-temperature ductility of these TGDDM–DDS epoxies.

(4) The lack of any heterogeneities on straining films of TGDDM–DDS (15 to 35 wt% DDS) epoxies in the electron microscope suggests that these glasses posses a uniform cross-link density distribution. However, TGDDM–DDS (10 to 15 wt% DDS) epoxies, which possess poorer network structures, break into ~2.5 nm diameter particles which are similar in size to the TGDDM epoxide molecule.

Acknowledgements

We wish to acknowledge Mr R. Helling (summer student, MDRL) for assistance in sample preparation and mechanical property measurements, Mr D. L. Fanter (MDRL) for assistance in sample preparation, and Dr D. R. Ulrich (AFOSR), Lt Col R. W. Haffner (AFOSR), Dr D. P. Ames (MDRL) and Dr C. J. Wolf (MDRL) for their support and encouragement of this work.

References

1. R. J. MORGAN and J. E. O'NEAL, *Polymer Preprints* **16** (1975) 610.
2. *Idem*, "Chemistry and Properties of Cross-linked Polymers," edited by S. S. Labana (Academic Press, New York, 1977) p. 289.
3. *Idem, J. Mater. Sci.* **12** (1977) 1966.
4. *Idem, J. Macromol. Sci. Phys.* **B15** (1978) 139.
5. D. KATZ and A. V. TOBOLSKY, *Polymer* **4** (1963) 417.
6. T. K. KWEI, *J. Polymer. Sci.* **A1** (1963) 2977.
7. A. S. KENYON and L. E. NIELSEN, *J. Macromol. Sci. -Chem.* **A3** (1969) 275.
8. R. P. KREAHLING and D. E. KLINE, *J. Appl. Polymer Sci.* **13** (1969) 2411.
9. J. P. BELL, *J. Polymer Sci. A-2* **8** (1970) 417.
10. T. MURAYAMA and J. P. BELL, *ibid.* **8** (1970) 437.
11. M. A. ACITELLI, R. B. PRIME and E. SACHER, *Polymer* **12** (1971) 335.
12. R. G. C. ARRIDGE and J. H. SPEAKE, *ibid.* **12** (1972) 443, 450.
13. P. V. SIDYAKIN, *Vysokomol. soyed.* **A14** (1972) 979.
14. T. HIRAI and D. E. KLINE, *J. Appl. Polymer. Sci.* **16** (1972) 3145.
15. R. B. PRIME and E. SACHER, *Polymer* **13** (1972) 455.
16. P. G. BABAYEVSKY and J. K. GILLHAM, *J. Appl. Polymer Sci.* **17** (1973) 2067.
17. T. HIRAI and D. E. KLINE, *J. Appl. Polymer Sci.* **17** (1973) 31.
18. E. SACHER, *Polymer* **14** (1973) 91.
19. D. A. WHITING and D. E. KLINE, *J. Appl. Polymer Sci.* **18** (1974) 1043.
20. J. K. GILLHAM, J. A. BENCI and A. NOSHAY, *ibid.* **18** (1974) 951.
21. J. F. CARPENTER, 21st National SAMPE Symposium, Los Angeles, April (1976).
22. L. T. PAPPALARDO, *J. Appl. Polymer Sci.* **21** (1977) 809.

23. T. S. CARSWELL, "Phenoplasts" (Interscience, New York, 1947).
24. T. G. ROCHOW and F. G. ROWE, *Anal. Chem.* **21** (1949) 261.
25. R. A. SPURR, E. H. ERATH, H. MYERS and D. C. PEASE, *Ind. Eng. Chem.* **49** (1957) 1839.
26. E. H. ERATH and R. A. SPURR, *J. Polymer Sci.* **35** (1959) 391.
27. T. G. ROCHOW, *Anal. Chem.* **33** (1961) 1810.
28. E. H. ERATH and M. ROBINSON, *J. Polymer Sci. C* **3** (1963) 65.
29. H. P. WOHNSIEDLER, *ibid.* (1963) 77.
30. D. H. SOLOMON, B. C. LOFT and J. D. SWIFT, *J. Appl. Polymer. Sci.* **11** (1967) 1593.
31. R. E. CUTHRELL, *ibid.* **11** (1967) 949.
32. A. N. NEVEROV, N. A. BIRKINA, Yu. V. ZHERDEV and V. A. KOZLOV, *Vysokomol. soyed.* **A10** (1968) 463.
33. G. NENKOV and M. MIKHAILOV, *Makromol. Chem.* **129** (1969) 137.
34. B. E. NELSON and D. T. TURNER, *J. Polymer Sci. (Phys. Ed.)* **10** (1972) 2461.
35. L. G. BOZVELIEV and M. G. MIHAJLOV, *J. Appl. Polymer Sci.* **17** (1973) 1963, 1973.
36. K. SELBY and L. E. MILLER, *J. Mater. Sci.* **10** (1975) 12.
37. R. J. MORGAN and J. E. O'NEAL, *Polymer Plast. Tech. Eng.* **5** (1975) 173.
38. M. V. MAIOROVA, M. M. MOGILEVICH, M. I. KARYAKINA and A. V. UDALOVA, *Vysokomol. soyed.* **A17** (1975) 471.
39. V. M. SMARTSEV, A. Ye. CHALYKH, S. A. NENAKHOV and A. T. SANZHAROVSKII, *ibid.* **A17** (1975) 836.
40. M. I. KARYAKINA, M. M. MOGILEVICH, N. V. MAIOROVA and A. V. UDALOVA, *ibid.* **A17** (1975) 466.
41. J. L. RACICH and J. A. KOUTSKY, *J. Appl. Polymer Sci.* **20** (1976) 2111.
42. K. SELBY and M. O. W. RICHARDSON, *J. Mater. Sci.* **11** (1976) 786.
43. J. A. MANSON, S. L. KIM, and L. H. SPERLING, "Influence of Crosslinking on the Mechanical Properties of High T_g Polymers," Technical Report AFML-TR-76-124 (1976).
44. S. L. KIM, M. D. SKIBO, J. A. MANSON, R. W. HERTZBERG and J. JANISZEWSKI, *Polymer Eng. Sci.* (in press).
45. G. PALMA, G. TALAMINI, M. TAVAN and M. CARENZA, *J. Polmer Sci. (Phys. Ed)* **15** (1977) 1537.
46. A. J. CHOMPFF, *Org. Coat. Plast. Chem. Preprints (ACS)* **36** (1976) 529.
47. A. H. WILLBOURN, *Polymer* **17** (1976) 965.
48. L. J. BROUTMAN and F. J. McGARRY, *J. Appl. Polymer. Sci.* **9** (1965) 609.
49. R. GRIFFITHS and D. G. HOLLOWAY, *J. Mater. Sci.* **5** (1970) 302.
50. R. L. PATRICK, W. G. GEHMAN, L. DUNBAR and J. A. BROWN, *J. Adhesion* **3** (1971) 165.
51. P. B. BOWDEN and J. A. DUKES, *J. Mater. Sci.* **7** (1972) 52.
52. R. L. PATRICK, "Treatise on Adhesion and Adhesive", Vol. 3, edited by R. L. Patrick (Dekker, New York, 1973) p. 163.
53. R. J. YOUNG and P. W. R. BEAUMONT, *J. Mater. Sci.* **10** (1975) 1343.
54. A. CHRISTIANSEN and J. B. SHORTALL, *ibid.* **11** (1976) 1113.
55. S. MOSTOVOY and E. J. RIPLING, *J. Appl. Polymer Sci.* **10** (1966) 1351.
56. *Idem, ibid.* **15** (1971) 611.
57. A. T. DiNENNEDETTO and A. D. WAMBACH, *Int. J. Polymer Mater.* **1** (1972) 159.
58. A. D. S. DIGGWA, *Polymer* **15** (1974) 101.
59. A. C. MEEKS, *ibid.* **15** (1974) 675.
60. W. D. BASCOM, R. L. COTTINGTON, R. L. JONES and P. PEYSER, *J. Appl. Polymer Sci.* **19** (1975) 2545.
61. P. G. BABAYEVSKII and Ye. B. TROSTYANSKAYA, *Vysokomol. soyed.* **A17** (1975) 906.
62. R. A. GLEDHILL and A. J. KINLOCH, *J. Mater. Sci.* **10** (1975) 1263.
63. Y. W. MAI and A. G. ATKINS, *ibid.* **10** (1975) 2000.
64. G. PRITCHARD and G. V. RHOADES, *Mater. Sci. Eng.* **26** (1976) 1.
65. D. L. FANTER, *Rev. Sci. Instrum.* **49** (1978) 1005.
66. H. EYRING, *J. Chem. Phys.* **4** (1936) 283.
67. P. B. BOWDEN, "The Physics of Glassy Polymers", edited by R. N. Haward (Wiley, New York, 1973) Ch. 5.
68. J. A. ROELTING, *Polymer* **6** (1965) 311.
69. D. L. HOLT, *J. Appl. Polymer Sci.* **12** (1968) 1653.
70. J. C. BAUWENS, C. BAUWENS-CROWET and G. HOMES, *J. Polymer Sci. A-2* **7** (1969) 1745.
71. R. A. DUCKETT, S. RABINOWITZ and I. M. WARD, *J. Mater. Sci.* **5** (1970) 909.
72. P. B. BOWDEN and S. RAHA, *Phil Mag.* **22** (1970) 463.
73. T. E. BRADY and G. S. Y. YEH, *J. Appl. Phys.* **42** (1971) 4622.
74. E. J. KRAMER, *J. Polymer Sci. (Phys. Ed.)* **13** (1975) 509.
75. E. PINK and J. D. CAMPBELL, *J. Mater. Sci.* **9** (1974) 665.
76. R. J. MORGAN and J. E. O'NEAL, *Polymer Plast. Tech. Eng.* **10** (1978) 49.
77. J. MURRAY and D. HULL, *Polymer* **10** (1969) 451.
78. S. RABINOWITZ, A. R. KRAUSE and P. BEARDMORE, *J. Mater. Sci.* **8** (1973) 11.
79. P. L. CORNES and R. N. HAWARD, *Polymer* **15** (1974) 149.
80. J. MURRAY and D. HULL, *J. Polymer Sci. A-2* **8** (1970) 1521.
81. P. BEAHAN, M. BEVIS and D. HULL, *J. Mater. Sci.* **8** (1972) 162.
82. M. J. DOYLE, *J. Polymer Sci. (Polymer Phys. Ed.)* **13** (1975) 127.
83. *Idem. J. Mater. Sci.* **10** (1975) 300.
84. J. HOARE and D. HULL, *J. Mater Sci.* **10** (1975) 1861.
85. F. ZANDEMAN, Publs. Scient. Tech. Minst. Air, Paris No. 291 (1954) Ch. IV.
86. S. B. NEWMAN and I. WOLOCK, *J. Appl. Phys.* **29** (1958) 49.
87. I. WOLOCK and S. B. NEWMAN, "Fracture Processes

in Polymeric Solids," edited by B. Rosen (Interscience, New York, (1964) Ch. IIc.
88. R. J. BIRD, J. MANN, G. POGANY and G. ROONEY, *Polymer* 7 (1966) 307.
89. R. P. KUSY and D. T. TURNER, *ibid.* **18** (1977) 391.
90. M. J. OWEN and R. G. ROSE, *J. Mater. Sci.* **10** (1975) 1711.
91. M. J. DOYLE, *ibid.* **10** (1975) 159.
92. H. EL-HAKEEM, G. P. MARSHALL, E. I. ZICHY and L. E. CULVER, *J. Appl. Polymer Sci.* **19** (1975) 3093.
93. D. L. LAINCHBURY and M. BEVIS, *J. Mater. Sci.* **11** (1976) 2222, 2235.
94. M. D. SKIBO, R. W. HERTZBERG and J. A. MANSON, *ibid.* **11** (1976) 479.
95. R. W. TRUSS and G. A. CHADWICK, *ibid.* **12** (1977) 1383.
96. R. P. KAMBOUR, *J. Polymer Sci.* **A3** (1965) 1713.
97. J. B. C. WU and J. C. M. LI, *J. Mater. Sci.* **11** (1976) 434.
98. P. B. BOWDEN and J. A. JUKES, *ibid.* **3** (1968) 183.
99. S. S. STERNSTEIN and L. ONGCHIN, *Polymer Preprints* **10** (1969) 1117.
100. R. N. HAWARD, B. M. MURPHY and E. F. T. WHITE, *J. Polymer Sci. A-2* **9** (1971) 801.
101. R. J. MORGAN and J. E. O'NEAL, *J. Polymer Sci. (Polymer Phys. Ed.)* **14** (1976) 1053.
102. D. HULL, *Acta Met.* **8** (1960) 11.
103. N. J. MILLS, *J. Mater. Sci.* **11** (1976) 363.
104. R. J. MORGAN and J. E. O'NEAL, unpublished data (1978).

Received 11 April and accepted 22 May 1978.